
Comparison of ^{11}C -Methionine and ^{18}F -FDG PET/CT for Staging and Follow-up of Pediatric Lymphoma

Sue C. Kaste¹⁻³, Scott E. Snyder¹, Monika L. Metzger^{2,4}, John T. Sandlund^{2,4}, Scott C. Howard⁵, Matthew Krasin⁶, and Barry L. Shulkin^{1,3}

¹Department of Diagnostic Imaging, St. Jude Children's Research Hospital, Memphis, Tennessee; ²Department of Oncology, St. Jude Children's Research Hospital, Memphis, Tennessee; ³Department of Radiology, University of Tennessee, School of Health Sciences, Memphis, Tennessee; ⁴Department of Pediatrics, University of Tennessee, School of Health Sciences, Memphis, Tennessee; ⁵School of Health Studies, University of Memphis, Memphis, Tennessee; and ⁶Department of Radiation Oncology, St. Jude Children's Research Hospital, Memphis, Tennessee

Methionine transport across plasma membranes occurs via the large amino acid transporter, which is overexpressed in malignant cells, leading to tracer accumulation within tumors. We investigated the uptake of ^{11}C -methionine (^{11}C -MET) in children and young adults with Hodgkin lymphoma (HL) or non-Hodgkin lymphoma (NHL) and compared the biodistribution of ^{11}C -MET PET/CT with that of ^{18}F -FDG PET/CT. **Methods:** Conducted under an investigational new drug authorization, we prospectively enrolled patients with newly diagnosed HL ($n = 19$) and NHL ($n = 2$) onto the Institutional Review Board-approved investigation of ^{11}C -MET PET/CT. After a minimum 4-h fast, patients received 740 MBq/1.7 m² (maximum, 740 MBq [20 mCi/1.7 m²; maximum, 20 mCi]) of ^{11}C -methionine intravenously. PET/CT was performed 5 min after injection from the vertex to thighs at 3 min per bed position. In a separate session, patients received 5.5 MBq/kg (maximum, 485 MBq [0.15 mCi/kg; maximum, 12 mCi]) of ^{18}F -FDG with imaging initiated approximately 1 h after radiopharmaceutical administration. All studies were reviewed by consensus of 2 senior imaging specialists. The presence of metabolic activity on baseline studies was compared among 17 nodal groups. **Results:** Eighteen patients (11 male; median age, 15.2 y; age range, 9.5–22.6 y) comprised the study cohort. All had paired ^{11}C -MET PET/CT and ^{18}F -FDG PET/CT studies at diagnosis. At baseline, 3 nodal groups demonstrating discordant metabolic activity by both ^{18}F -FDG PET/CT and ^{11}C -MET PET/CT were Waldeyer's ring, paraaortic region, and the liver. All others were found to have concordant metabolic activity. Normal intense ^{11}C -MET uptake in the pancreas and liver reduced sensitivity for disease detection in these regions. At follow-up, 14 of 15 study pairs had concordant results. **Conclusion:** ^{11}C -MET uptake is elevated in most regions involved with lymphoma at diagnosis and follow-up. Its utility in the abdomen is limited by uptake in normal structures.

Key Words: lymphoma; methionine; fluorodeoxyglucose; Hodgkin disease

J Nucl Med 2017; 58:419–424

DOI: 10.2967/jnumed.116.178640

Protein formation is integral for cellular growth and replication. Methionine is a naturally occurring essential amino acid critical not only for protein formation but also for phospholipid synthesis through intermediate compounds. When labeled with ^{11}C , a radioactive isotope of the naturally occurring carbon-12, the distribution of methionine can be determined noninvasively using a PET camera. Imaging with ^{11}C -methionine (^{11}C -MET) has proven useful for a variety of neoplasms, because of its increased uptake via large amino acid transporter (LAT1) (1).

Despite the interest in ^{11}C -methionine imaging for brain tumors, results of few other investigations regarding the role of this agent in tumor imaging are available. Thus, we sought to characterize the activity of LAT1 in pediatric and young adult patients with lymphoma, assess the biodistribution of the tracer in tumor sites, and compare with ^{18}F -FDG PET/CT used for staging and response (2).

^{18}F -FDG is a valuable radiopharmaceutical tracer to stage, monitor response to therapy, and detect relapsed disease in lymphomas occurring in both adults and children. Nevertheless, ^{18}F -FDG has limitations to its use (3). ^{18}F -FDG uptake largely reflects glucose transport, which is increased not only in many tumors, but also in common nonneoplastic conditions such as infections and inflammation. Thus, ^{18}F -FDG is a sensitive tracer for detecting increased glucose metabolism, but nonneoplastic etiologies may mimic tumor uptake, thus reducing specificity when screening for cancer (3–5). There is therefore a need for more tracers with greater specificity for malignancy.

We evaluated the activity of LAT1 in sites of lymphoma using the tracer ^{11}C -MET as a transporter substrate. We examined the potential usefulness of PET/CT imaging with ^{11}C -MET in the evaluation of children and young adults with lymphoma in initial disease staging, and in response to therapy, and compared response assessment of disease between ^{11}C -MET and ^{18}F -FDG.

MATERIALS AND METHODS

Our investigation was initiated after obtaining Institutional Review Board approval and was conducted under an investigational new drug authorization. Data management complied with the Health Information Portability and Accountability Act of 2013.

Recruitment Process

With agreement from the primary institutional attending physician and on determination of the patient's eligibility, the patient was approached for enrollment. Patients included in this report were recruited from

Received Jun. 8, 2016; revision accepted Aug. 22, 2016.

For correspondence or reprints contact: Sue C. Kaste, Department of Diagnostic Imaging, 262 Danny Thomas Place, MSN #220, Memphis, TN 38105.

E-mail: sue.kaste@stjude.org

Published online Sep. 8, 2016.

COPYRIGHT © 2017 by the Society of Nuclear Medicine and Molecular Imaging.

August 2009 through November 2013. Patients of any age were eligible for enrollment if they had known or suspected lymphoma, had scheduled clinical imaging evaluations that included ^{18}F -FDG PET/CT within 4 wk of entry, and had provided an informed consent form (signed by participant, parent, or guardian) and assent according to the guidelines of the Institutional Review Board. The Institutional Review Board approved this study. To be evaluable, newly diagnosed patients with Hodgkin lymphoma (HL) or non-Hodgkin lymphoma (NHL) could not have started therapy before the initial ^{11}C -MET PET/CT or ^{18}F -FDG PET/CT scans (Fig. 1).

Exclusion criteria included pregnancy, treatment having already started, and the inability or unwillingness of research participant, parent, or legal guardian/representative to give written informed consent; female participants could not be breast feeding because of the theoretic potential of harm to the infant from exposure to ionizing radiation from the radiopharmaceutical.

Technical Factors for ^{11}C -MET

Participants fasted for at least 4 h before imaging. Patients then received 740 MBq (20 mCi) of ^{11}C -MET per 1.7 m² of body surface area (maximum prescribed dose, 740 MBq [20 mCi]) intravenously. Transmission CT image acquisitions, for attenuation correction and lesion localization, and PET image acquisitions were initiated approximately 5 min later using a Discovery LS PET/CT or a Discovery 690 PET/CT system (GE Healthcare). Images from the top of the head to the mid thighs were acquired at 3 min per bed position.

Technical Factors for ^{18}F -FDG

After a minimum of 4 h of fasting, blood glucose was assessed before ^{18}F -FDG injection. If blood glucose was determined to be within normal limits, 5.5 MBq/kg (0.15 mCi/kg) of ^{18}F -FDG (maximum, 444 MBq [12 mCi]) were injected intravenously. Patients were kept in a quiet, dark room after injection and were instructed to relax with their arms at their sides in a recumbent position. Approximately 1 h later, transmission CT images, for attenuation correction and lesion localization, and PET emission images were acquired using a Discovery LS PET/CT or a GE Discovery 690 PET/CT system (GE Healthcare). Images were

obtained from the top of the head through the feet at 5 min per bed position on the Discovery LS in 2-dimensional mode and 3–5 min per bed position on the GE Discovery 690 PET/CT in 3-dimensional mode.

The scans were typically obtained an average of 4 d between the 2 studies (median, 1.5 d). For those for whom the studies were performed on the same day, ^{11}C -MET PET/CT was performed first, with injection of ^{18}F -FDG administered 2 h after ^{11}C -MET. ^{18}F -FDG PET/CT scans were thus obtained 3 h after the injection of ^{11}C -MET, at which time less than 0.2% of the injected dose of ^{11}C -MET would remain.

Technical Factors for CT Obtained for Attenuation Correction and Lesion Localization

CT acquisition parameters included a slice thickness of 0.5 cm, tube rotation of 0.8 s, table speed of 1.5 cm/rotation, and pitch of 1.5:1, at 120 kV and 90 mA, with dose modulation. PET and CT data were reconstructed into multiplanar cross-sectional images using standard vendor-supplied software and displayed on a nuclear medicine workstation (Hermes Medical Solutions) for analysis.

Imaging Review

^{18}F -FDG and ^{11}C -MET PET/CT data were all reviewed by a nuclear medicine physician and a pediatric radiologist, each with more than 25 y of experience, and scored by consensus. To avoid bias, studies were reviewed in groups by study type (i.e., all ^{18}F -FDG PET/CT images were reviewed as 1 group, and 4 wk later ^{11}C -MET PET/CT images were reviewed as a separate group). Study review was performed without knowledge of clinical findings or the results of other studies of each patient.

Individual lymph nodes; nodal masses; and lung, skeletal, and solid organ lesions were coded as positive if the metabolic activity exceeded that of adjacent background tissues. Individual lymph nodes were then classified into 17 groups: Waldeyer's ring (including nasopharyngeal, tonsillar, and base of tongue), right and left neck (including supraclavicular nodal groups), right and left axilla, mediastinum (including epicardial, internal mammary, diaphragmatic nodes), right and left pulmonary hila, abdominal (including paraaortic, porta hepatic, retroperitoneal, mesenteric, and celiac nodal groups), liver, spleen (including splenic hilar), and pelvic (right and left iliac, and right and left inguinal/femoral). Lung, bone, or bone marrow involvement was each classified as individual sites. The range, median, and maximum SUVs were recorded for each site for both radiopharmaceuticals.

RESULTS

Staging

Between August 2009 and the end of November 2013, 21 of 85 (25%) potentially eligible patients with HL ($n = 67$) or NHL ($n = 18$) were enrolled (median age, 15.2 y; age range, 9.5–22.6 y). Eleven patients were boys. Eighteen patients with paired studies were evaluable at diagnosis, because 1 patient had to be excluded due to extensive uptake in brown adipose tissue and 2 had missing paired studies. Of this population, 17 had a diagnosis of HL and 1 of NHL.

At the time of diagnosis, 14 of 17 regions evaluated showed concordant uptake of both tracers (Figs. 2 and 3). Three nodal groups demonstrated discordant metabolic activity between ^{18}F -FDG and ^{11}C -MET: Waldeyer's ring, paraaortic region, and liver (Fig. 4). Intense ^{11}C -MET uptake in the pancreas and liver interfered with disease detection in the liver, porta hepatis, and upper retroperitoneum (Table 1; Fig. 4).

The number of abnormal sites of metabolic activity was nearly identical for both tracers except for nearly one-third more foci being identified within the abdomen with ^{18}F -FDG than with ^{11}C -MET (Table 2). Further, the median intensity of activity as represented by

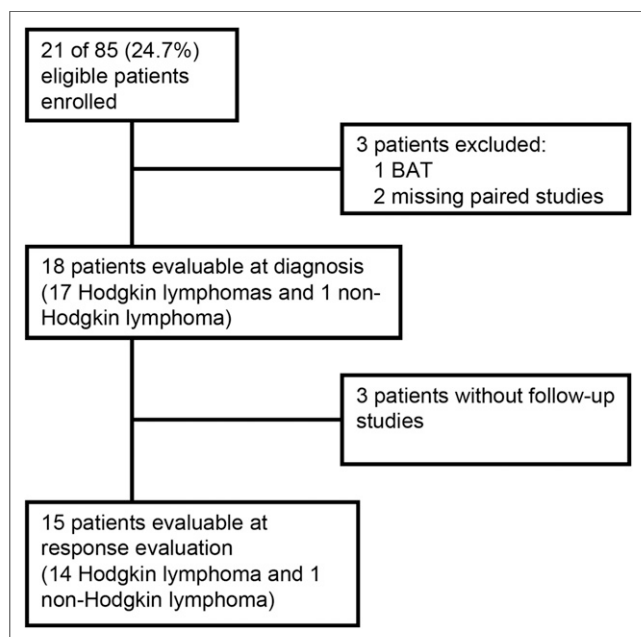


FIGURE 1. Consort diagram. BAT = brown adipose tissue.

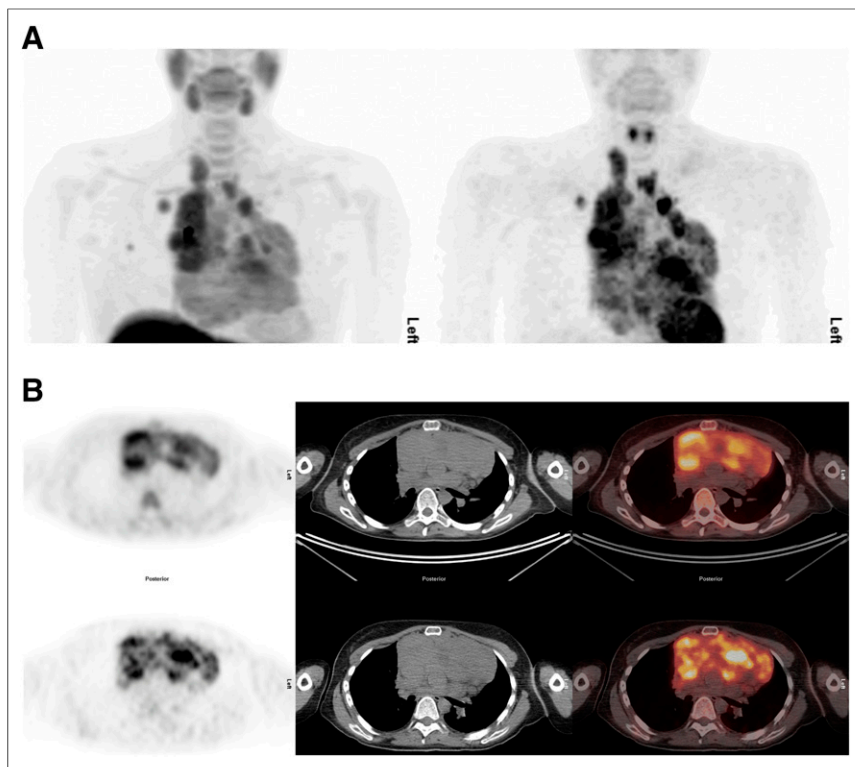


FIGURE 2. A 22-y-old woman with mediastinal lymphadenopathy. Biopsy showed nodular sclerosing HL. (A) Maximum-intensity-projection images (^{11}C -MET left, ^{18}F -FDG right) show intense though variable uptake of both tracers throughout mediastinal masses. Small focus of ^{11}C -MET appearing over right midchest lay within tubing leading to the central line. Images are normalized to SUV_{max} of 5.0 for ^{11}C -MET and 8.0 for ^{18}F -FDG. (B) Transverse images (left column, PET; middle column, attenuation-correction CT; right column, fusion) through lower aspect of mediastinal mass (^{11}C -MET top, ^{18}F -FDG bottom). Uptake of both tracers is slightly heterogeneous, but regional distribution is largely concordant. Images are normalized to SUV_{max} of 5.0 for ^{11}C -MET and 8.0 for ^{18}F -FDG.

SUVs was similar in most regions. However, the range of uptake was greater with ^{18}F -FDG, particularly in the mediastinum, hila, and abdomen in which the SUV_{max} was 2–3 times greater than with ^{11}C -MET (Table 2).

Restaging

All patients were treated according to institutional guidelines or enrolled on protocol when available. Of the 18 enrolled patients, the patient with diffuse large B cell lymphoma (NHL) was treated according to previously published standard therapy (4). Eleven

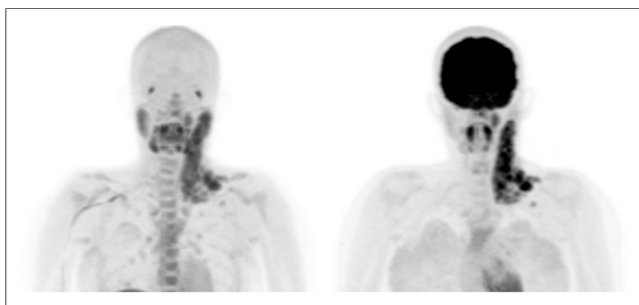


FIGURE 3. A 17-y-old girl with mixed cellularity HL. Maximum-intensity-projection images (^{11}C -MET left, ^{18}F -FDG right) show intense uptake in left cervical and supraclavicular masses. Images are normalized to SUV_{max} of 7.0 for ^{11}C -MET and 5.0 for ^{18}F -FDG.

HL patients were treated with a modified Stanford V protocol (5,6), 4 according to a modified German Pediatric Oncology/Hematology-Hodgkin Disease 2002 regimen (7), 1 according to German Hodgkin Study Group-14 trial (8), and 1 with stage IA lymphocyte predominant HL was observed without further treatment after complete excision of the affected lymph node. After 8 wk of therapy, paired follow-up imaging was available for 15 patients (1 patient underwent ^{11}C -methionine follow-up imaging but lacked the corresponding ^{18}F -FDG study, and 2 patients declined further participation) (Fig. 5). In 14 patients, uptake of ^{11}C -MET and ^{18}F -FDG was concordant. In 4 patients, both ^{18}F -FDG and ^{11}C -MET remained positive, and in 10 patients abnormal uptake of both tracers resolved. In 1 patient, metabolic activity was minimally discordant where the ^{18}F -FDG study had normalized but the ^{11}C -MET study remained slightly positive in the right internal mammary and left infraclavicular nodal regions. Subsequent review of the studies in combination indicated only slight discrepancy in uptake, likely due to lower mediastinal background in ^{11}C -MET images. This patient is alive and well without relapse more than 3 y from diagnosis. None of the patients in this study had documented bone marrow disease.

Outcomes

There were no adverse events associated with the study, and all patients remain alive at a median of 3 y (range, 1.0–5.7 y) from

diagnosis. Three patients developed disease recurrence at a median of 0.4 y (range, 0.3–2.3 y), and 1 patient with HL developed a secondary NHL (diffuse large B cell lymphoma) at 1.4 y from original diagnosis; all patients have been seen in our institution within the last 6 mo.

DISCUSSION

Within the neck and axilla, the number of abnormal foci independently identified without reference to the other studied tracer was nearly identical for ^{11}C -MET and ^{18}F -FDG. This finding may be due to the low background uptake of either tracer in the neck and axilla, facilitating detection of abnormal foci, as well as the most common sites of disease in this patient population. Nearly 3 times as many abnormal foci were discovered within the abdomen and pelvis with ^{18}F -FDG than with ^{11}C -MET, reflecting the intense, normal uptake of ^{11}C -MET within the liver and pancreas, which may obscure foci of abnormal uptake, as also reported by Sutinen et al. in a cohort of 55 adult patients with lymphoma (9). Too few lesions were noted in the spleen to allow for comparison of detection between ^{18}F -FDG and ^{11}C -MET. Except for the axilla and pelvis, median uptake was about 1.5–2.5 greater with ^{18}F -FDG than with ^{11}C -MET.

The value of determining metabolically active disease regardless of the anatomic characteristics of lymphoma has been well-established (10). ^{18}F -FDG serves as a sensitive but not entirely tumor-specific agent widely used for detection and response evaluation

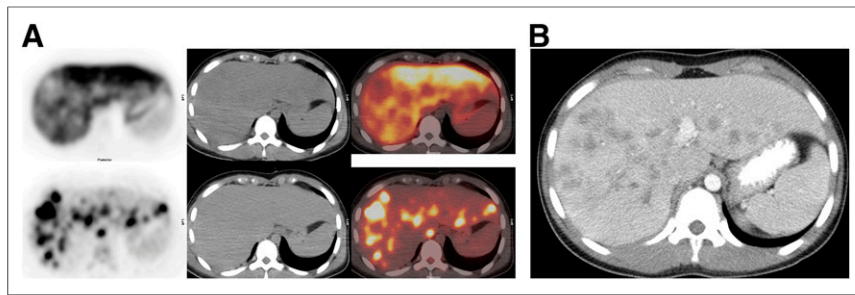


FIGURE 4. A 15-y-old girl with widespread nodular sclerosing HL. (A) Transverse images (left column, PET; middle column, attenuation-correction CT; right column, fusion) through upper aspect of liver (^{11}C -MET top, ^{18}F -FDG bottom). Intense uptake of ^{11}C -MET renders hepatic metastases to appear as areas of low activity in comparison to normal liver. Hepatic metastases are quite discernible on ^{18}F -FDG images. Images are normalized to SUV_{max} of 15.0 for ^{11}C -MET and 7.0 for ^{18}F -FDG. (B) Contrast-enhanced CT scan through same region shows many areas of low attenuation consistent with extensive liver involvement.

of lymphomas, but its lower specificity for malignant disease may complicate study interpretation (11). ^{18}F -FDG has been used to identify most lymphomas although slightly fewer sites in indolent lymphomas were detected using ^{18}F -FDG than ^{67}Ga scintigraphy (12). The authors further reported that ^{11}C -MET showed all sites of lymphoma identified by ^{18}F -FDG, which contrasts with our finding of ^{11}C -MET identifying fewer sites of metabolically active disease in the abdomen and pelvis than ^{18}F -FDG. The ability of ^{11}C -MET to distinguish between high- and low-grade lymphomas has not been conclusively established (13,14).

tients with NHL, 1 patient with HL) peaked about 10 min after injection and remained nearly constant for at least 30 min. The authors compared methods using blood samples with DAR (differential absorption ratio, now referred to as SUV) obtained using images only and found they were highly correlated ($r = 0.875$). They concluded that the DAR gave almost the same result as the more complicated dynamic analyses using blood sampling (17). In our article, we chose SUV for semiquantitative comparisons between tumor uptake of ^{11}C -MET and ^{18}F -FDG, recognizing that comparison between tracers reflects multiple factors, including the

Most studies describing amino acid tracers in oncologic imaging using ^{11}C -MET have been for central nervous system neoplasms, and its role in clinical management has been described (15). ^{11}C -MET has also been explored for its potential utility in patients with lymphomas (16). Nuutinen et al. found that ^{11}C -MET accumulated in 31 of 32 lymphomas (27/28 NHL, 4/4 HL), the exception being a superficial skin lesion. The sensitivity was 97%, and there were no false-positive findings. ^{11}C -MET accumulation was high in all grades of lymphoma. When kinetic analysis was performed, the difference in ^{11}C -MET uptake between high-, intermediate-, and low-grade tumors was statistically significant. Yoshida showed that ^{11}C -MET activity in lymphomas (6 patients with NHL, 1 patient with HL) peaked about 10 min after injection and remained nearly constant for at least 30 min. The authors compared methods using blood samples with DAR (differential absorption ratio, now referred to as SUV) obtained using images only and found they were highly correlated ($r = 0.875$). They concluded that the DAR gave almost the same result as the more complicated dynamic analyses using blood sampling (17). In our article, we chose SUV for semiquantitative comparisons between tumor uptake of ^{11}C -MET and ^{18}F -FDG, recognizing that comparison between tracers reflects multiple factors, including the

TABLE 1
Comparison of Number of Cases at Study Entry Demonstrating Metabolic Activity by ^{18}F -FDG and ^{11}C -MET by Anatomic Regions

| Group | ^{18}F -FDG-positive cases | ^{11}C -MET-positive cases |
|--|-------------------------------------|-------------------------------------|
| Neck (includes periclavicular, periauricular, submental) | | |
| Right | 10 | 10 |
| Left | 15 | 15 |
| Waldeyer's ring (includes nasopharyngeal, tonsillar, tongue base) | 2 | 1 |
| Axilla (includes pectoral nodes) | | |
| Right | 6 | 6 |
| Left | 7 | 7 |
| Mediastinum (includes epicardial, internal mammary, diaphragmatic) | 14 | 14 |
| Lung | 1 | 1 |
| Hilum | | |
| Right | 6 | 6 |
| Left | 7 | 7 |
| Paraaortic (includes porta hepatic, retroperitoneal, celiac) | 7 | 2 |
| Liver | 2 | 0 |
| Spleen | 1 | 1 |
| Mesenteric | 0 | 0 |
| Iliac | | |
| Right | 4 | 4 |
| Left | 3 | 3 |
| Inguinal/femoral | | |
| Right | 4 | 4 |
| Left | 4 | 4 |

TABLE 2
Comparison of Metabolic Activity (SUV) by ^{11}C -MET and ^{18}F -FDG by Anatomic Region

| Group | Tracer | No. of abnormal regions | SUV median | SUV range |
|-------------|----------------------|-------------------------|------------|-----------|
| Neck | ^{11}C -MET | 28 | 4.6 | 1.3–9.3 |
| | ^{18}F -FDG | 27 | 4.7 | 3.1–16.1 |
| Axilla | ^{11}C -MET | 12 | 5.6 | 2.0–10.1 |
| | ^{18}F -FDG | 12 | 4.6 | 2.4–5.9 |
| Mediastinum | ^{11}C -MET | 14 | 4.9 | 1.3–7.4 |
| | ^{18}F -FDG | 14 | 11.1 | 3.0–15.3 |
| Hila | ^{11}C -MET | 11 | 4.1 | 2.6–7.1 |
| | ^{18}F -FDG | 11 | 6.1 | 3.9–13.4 |
| Spleen | ^{11}C -MET | 2 | 5.2 | 4.8–5.5 |
| | ^{18}F -FDG | 3 | 4.6 | 3.9–10.3 |
| Abdomen | ^{11}C -MET | 6 | 5.0 | 2.1–7.5 |
| | ^{18}F -FDG | 9 | 6.4 | 3.0–14.6 |
| Pelvis | ^{11}C -MET | 8 | 5 | 2.4–8.9 |
| | ^{18}F -FDG | 8 | 4.0 | 3.0–7.1 |

injection to imaging interval, the background biodistribution of the tracers, and the tumor avidity for the particular agent.

Ogawa et al. (18) used ^{11}C -MET in the follow-up of radiotherapy of primary central nervous system lymphoma. Nine patients with primary brain lymphoma and 1 patient with secondary central nervous system involvement were the subjects. As has been documented in primary central nervous system tumors, ^{11}C -MET uptake was higher in tumor than in uninvolved brain before therapy. In most patients, the extent of ^{11}C -MET uptake correlated well with contrast enhancement on MRI and CT, but in 2 patients, the extent of ^{11}C -MET uptake was larger than the areas of enhancement on CT and MRI. The uptake intensity of ^{11}C -MET declined after radiotherapy, but the extent of uptake was larger than the areas of enhancement on CT and MR in 8 patients. One patient had a recurrence at the site of residual ^{11}C -MET uptake after radiotherapy. Uptake in the tumor declined from an SUV of 4.3 ± 1.8 to an SUV of 1.9 ± 0.5 after radiotherapy. Importantly, the uptake in normal, uninvolved brain did not change (SUV of 1.4 ± 0.3 at baseline and 1.6 ± 0.3 after radiotherapy). As do others, the authors believed that a larger area of ^{11}C -MET uptake compared with contrast enhancement

on MR and CT indicated tumor infiltration beyond the borders of contrast enhancement. The authors concluded that ^{11}C -MET PET might be useful for detecting residual tumor after treatment and for early diagnosis of recurrent intracranial disease.

Methionine and other neutral amino acids with large, branched, or aromatic side chains, including phenylalanine and tyrosine, are transported into cells by LAT1 (19). LAT1 is also the transporter for amino acid–related molecules such as L-dopa, thyroxine, and triiodothyronine as well as the chemotherapeutic agent melphalan (L-phenylalanine mustard) (20). LAT1 is found in the brain, placenta, and liver, and it is overexpressed in many types of tumors including gliomas (21). Inhibition of LAT1 has been reported to have antitumor activity in vitro and in vivo (20). If effective therapies using LAT1 inhibitors are developed, it is possible that tracers that examine the functional integrity of LAT1, such as ^{11}C -MET or other amino acids and amino acid derivatives such as ^{18}F -FET (fluoroethyl tyrosine) (22), could serve as a method to assess antitumor efficacy.

Other radiotracers have been used to assess the activity of lymphomas (23). ^{18}F -FLT is the thymidine analog 3'-deoxy-3'- ^{18}F -fluorothymidine (24–26). Buck demonstrated that in a mouse model, ^{18}F -FLT showed a response to chemotherapy before changes in tumor size occurred. Buchmann showed that ^{18}F -FLT could be used to image both aggressive and indolent NHL. However, there was substantial normal accumulation in bone marrow and liver, which, similar to ^{11}C -MET, may interfere with disease assessment in these organs. Kasper examined 15 patients with HL and 33 with NHL who had residual masses larger than 2 cm after treatment. Both ^{18}F -FDG and ^{18}F -FLT were useful in distinguishing between patients with long or short overall survivals, predicting those at greater risk for disease relapse. Those patients with ^{18}F -FDG- or ^{18}F -FLT-negative scans were found to have improved survival compared with those whose scans remained positive after

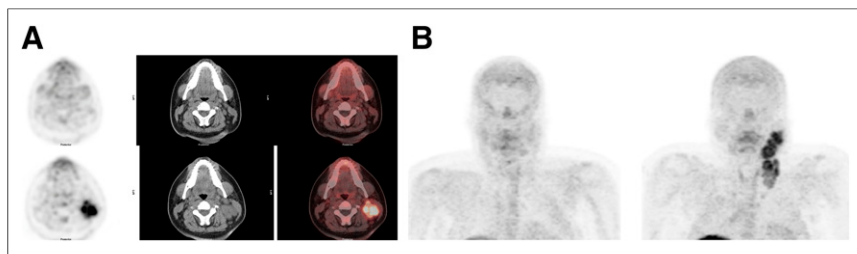


FIGURE 5. A 16-y-old boy with mixed cellularity HL. ^{11}C -MET images after 8 wk of chemotherapy and at presentation. (A) Transverse images after 8 wk of chemotherapy (top row) and at presentation (bottom row) (left column, PET; middle column, attenuation-correction CT; right column, fusion). There has been resolution of abnormal ^{11}C -MET activity and considerable reduction in size in left cervical sites. (B) Maximum-intensity-projection images after 8 wk of chemotherapy (left) and at presentation (right) show that activity within neck has become normal during treatment.

therapy. The authors concluded that combining ^{18}F -FLT with ^{18}F -FDG in this clinical situation provided no additional information.

CONCLUSION

We have found that most sites of tumor involvement in children with HL and NHL are well visualized using ^{11}C -MET PET/CT. Tumor sites in the neck and chest were particularly evident because of the low background uptake of methionine in these areas. However, within the abdomen, we found that uptake in the liver was more intense than tumor. Thus, sites of tumor appeared as cold spots. Furthermore, we expect that normal bone marrow uptake will interfere with detection of tumor bone marrow involvement. Tumor uptake declined markedly with treatment, in most patients resolving in 8 wk, indicating that the activity of LAT1 decreases with effective tumor treatment. Thus, amino acid imaging using ^{11}C -MET demonstrates consistent overexpression of LAT1 in pediatric lymphomas at diagnosis and subsequent decline in expression in most patients during therapy, similar to glucose transporters.

DISCLOSURE

No other potential conflict of interest relevant to this article was reported.

REFERENCES

- Miyazawa H, Arai T, Iio M, Hara T. PET imaging of non-small-cell lung carcinoma with carbon-11-methionine: relationship between radioactivity uptake and flow-cytometric parameters. *J Nucl Med.* 1993;34:1886–1891.
- Harris SM, Davis JC, Snyder SE, et al. Evaluation of the biodistribution of ^{11}C -methionine in children and young adults. *J Nucl Med.* 2013;54:1902–1908.
- Beadsmoore C, Newman D, MacIver D, Pawaroo D. Positron emission tomography computed tomography: a guide for the general radiologist. *Can Assoc Radiol J.* 2015;66:332–347.
- Patte C, Auperin A, Gerrard M, et al. Results of the randomized international FAB/LMB96 trial for intermediate risk B-cell non-Hodgkin lymphoma in children and adolescents: it is possible to reduce treatment for the early responding patients. *Blood.* 2007;109:2773–2780.
- Advani RH, Hoppe RT, Baer D, et al. Efficacy of abbreviated Stanford V chemotherapy and involved-field radiotherapy in early-stage Hodgkin lymphoma: mature results of the G4 trial. *Ann Oncol.* 2013;24:1044–1048.
- Edwards-Bennett SM, Jacks LM, Moskowitz CH, et al. Stanford V program for locally extensive and advanced Hodgkin lymphoma: the Memorial Sloan-Kettering Cancer Center experience. *Ann Oncol.* 2010;21:574–581.
- Mauz-Körholz C, Hasenclever D, Dorffel W, et al. Procarbazine-free OEPA-COPDAC chemotherapy in boys and standard OPPA-COPP in girls have comparable effectiveness in pediatric Hodgkin's lymphoma: the GPOH-HD-2002 study. *J Clin Oncol.* 2010;28:3680–3686.
- von Tresckow B, Plutschow A, Fuchs M, et al. Dose-intensification in early unfavorable Hodgkin's lymphoma: final analysis of the German Hodgkin Study Group HD14 trial. *J Clin Oncol.* 2012;30:907–913.
- Sutinen E, Jyrkkio S, Varpula M, et al. Nodal staging of lymphoma with whole-body PET: comparison of. *J Nucl Med.* 2000;41:1980–1988.
- Barrington SF, Mikhael NG, Kostakoglu L, et al. Role of imaging in the staging and response assessment of lymphoma: consensus of the International Conference on Malignant Lymphomas Imaging Working Group. *J Clin Oncol.* 2014;32:3048–3058.
- Culverwell AD, Scarsbrook AF, Chowdhury FU. False-positive uptake on 2- ^{18}F -fluoro-2-deoxy-D-glucose (FDG) positron-emission tomography/computed tomography (PET/CT) in oncological imaging. *Clin Radiol.* 2011;66:366–382.
- Tsukamoto N, Kojima M, Hasegawa M, et al. The usefulness of ^{18}F -fluorodeoxyglucose positron emission tomography (^{18}F -FDG-PET) and a comparison of ^{18}F -FDG-PET with ^{67}Ga gallium scintigraphy in the evaluation of lymphoma: relation to histologic subtypes based on the World Health Organization classification. *Cancer.* 2007;110:652–659.
- Leskinen-Kallio S, Ruotsalainen U, Nagren K, Teras M, Joensuu H. Uptake of carbon-11-methionine and fluorodeoxyglucose in non-Hodgkin's lymphoma: a PET study. *J Nucl Med.* 1991;32:1211–1218.
- Rodriguez M, Rehn S, Ahlstrom H, Sundstrom C, Glimelius B. Predicting malignancy grade with PET in non-Hodgkin's lymphoma. *J Nucl Med.* 1995;36:1790–1796.
- Heiss WD. Clinical impact of amino acid PET in gliomas. *J Nucl Med.* 2014;55:1219–1220.
- Nuutinen J, Leskinen S, Lindholm P, et al. Use of carbon-11 methionine positron emission tomography to assess malignancy grade and predict survival in patients with lymphomas. *Eur J Nucl Med.* 1998;25:729–735.
- Yoshida H, Yoshikawa K, Imazeki K, et al. Correlation analysis between Patlak plot and DAR using ^{11}C -methionine PET [in Japanese]. *Nippon Igaku Hoshasen Gakkai Zasshi.* 1995;55:582–586.
- Ogawa T, Kanno I, Hatazawa J, et al. Methionine PET for follow-up of radiation therapy of primary lymphoma of the brain. *Radiographics.* 1994;14:101–110.
- Fuchs BC, Bode BP. Amino acid transporters ASCT2 and LAT1 in cancer: partners in crime? *Semin Cancer Biol.* 2005;15:254–266.
- Oda K, Hosoda N, Endo H, et al. L-type amino acid transporter 1 inhibitors inhibit tumor cell growth. *Cancer Sci.* 2010;101:173–179.
- Okubo S, Zhen HN, Kawai N, Nishiyama Y, Haba R, Tamiya T. Correlation of L-methyl- ^{11}C -methionine (MET) uptake with L-type amino acid transporter 1 in human gliomas. *J Neurooncol.* 2010;99:217–225.
- Dunet V, Rossier C, Buck A, Stupp R, Prior JO. Performance of ^{18}F -fluoroethyl-tyrosine (^{18}F -FET) PET for the differential diagnosis of primary brain tumor: a systematic review and metaanalysis. *J Nucl Med.* 2012;53:207–214.
- Wang R, Zhu H, Chen Y, et al. Standardized uptake value based evaluation of lymphoma by FDG and FLT PET/CT. *Hematol Oncol.* 2014;32:126–132.
- Buchmann I, Neumaier B, Schreckenberger M, Reske S. [^{18}F]3'-deoxy-3'-fluorothymidine-PET in NHL patients: whole-body biodistribution and imaging of lymphoma manifestations—a pilot study. *Cancer Biother Radiopharm.* 2004;19:436–442.
- Buck AK, Kratochwil C, Glatting G, et al. Early assessment of therapy response in malignant lymphoma with the thymidine analogue [^{18}F]FLT. *Eur J Nucl Med Mol Imaging.* 2007;34:1775–1782.
- Kasper B, Egerer G, Gronkowski M, et al. Functional diagnosis of residual lymphomas after radiochemotherapy with positron emission tomography comparing FDG- and FLT-PET. *Leuk Lymphoma.* 2007;48:746–753.